Characterization of Insulation Material Parameters in Low-Voltage Electrical Machines

N. Driendl, F. Pauli and K. Hameyer, *Senior Member, IEEE*

2022 International Conference on Electrical Machines (ICEM) | 978-1-6654-1432-6/22/$31.00 ©2022 IEEE | DOI: 10.1109/ICEM51905.2022.9910865

***Abstract*—In inverter-driven low-voltage electrical machines, the insulation system is stressed by steep voltage slopes. In many applications, the use of silicon carbide-based semiconductors and an increase in the DC link voltage are desired. These trends reinforce the risk of partial discharges which are mainly triggered by high electric fields. Material parameter such as the permittivity and the thickness of the insulation layer influence the electric field inside the insulation system. To determine the permittivity, capacity measurements are carried out on enameled wires. Besides, the cross-section of the wires is analyzed to measure the insulation thickness allowing the calculation of the permittivity based on a cylinder capacitor geometry. To study the influence of these parameters, the *Townsend* equation is used to determine the expected partial discharge inception voltage. By comparing the simulation results to partial discharge measurements on twisted pair samples, the secondary-electron-emission coefficient can be determined.**

***Index Terms*—electrical machine, insulation system, insulation material**

I. Introduction

The insulation system of low-voltage electrical machines consists of various components. Usually, the conductors are insulated by enamel providing the turn-to-turn insulation. The phase-to-phase insulation (slot divider or phase separator) and the slot insulation (slot liner) is commonly made of papers or flexible laminates. Additionally, impregnation or potting can be used to reduce air inclusions inside the insulation system. The impregnation also improves the heat dissipation and mechanical strength [1].

The design of the insulation system is made according to certain constrains. Besides the thermal class, the mechanical strength and the resistance to environmental conditions is of great interest. Ensuring the partial discharge-free operation is a crucial part in the design process. Partial discharges are deterioration processes yielding premature failure of the insulation system. Such processes usually occur in air-filled voids inside the insulation system, if the dielectric strength of the air is exceeded [2]–[4]. The external electric voltage from which partial discharges occur, is named partial discharge inception voltage (PDIV). In low-voltage electrical machines, partial discharges must be avoided during the whole service life, according to DIN EN 60034-18-41 [5].

In inverter-driven electrical machines, the insulation system is exposed to steep voltage slopes leading to an overvoltage at the machine's terminals [2], [6]–[8]. Besides the external electrical voltage, the electric field inside air-filled voids depends on the material parameters of the insulation. The permittivity of the insulation material is a measure of the electric polarizability. A higher value of the permittivity as well as a thinner insulation layer leads to an increased electric field inside the air increasing the risk of partial discharge inception.

The turn-to-turn insulation is often focused as it is usually regarded to be the weakest part of the insulation system [9], [10], i.e. the part where partial discharges are most likely to occur. Therefore, special attention is paid on the enamel of the conductors. From the designer's point of view, the insulation layer should be as thin as possible to achieve a high copper filling factor but sufficiently thick to ensure the absence of partial discharges. Frequently used polymeric materials are for example polyetherimide (PEI), polyesterimide (PESI) and polyamide-imide (PAI) [11], [12]. In some applications, polyether ether ketone (PEEK) is used. In safety-critical applications, such as More Electric Aircraft, the use of so called corona-resistant insulation layers is discussed. These polymer-based materials additionally consist of inorganic nano-fillers increasing the lifetime under partial discharge exposure [13]–[15].

In the design process of the insulation system, the PDIV is calculated by using simulation models based on the Finite-Element-Method (FEM) in combination with physical models describing the gas discharge process [16]–[18]. In this work, the *Townsend* criterion is used. As stated in [19], measuring the permittivity of the insulation material improves the accuracy of the calculation. Usual manufacturer information consists of the following data:

- number of insulation layers,
- insulation material and
- grade of insulation layer.

The latter information refers to the insulation thickness in a specific range. The exact value is usually unknown as well as the permittivity. Without characterization of the insulation material, only assumptions can be made. With the provided method in this paper, it is possible to study the influence of the insulation material on the PDIV and compare different types of wires.

In the first step, the capacity of the insulation layer of three different wires is measured. After that, the cross-section of the enameled wires is analyzed. Subsequently, the results are used to set up a simulation model of the different geometries. With this model, the influence of the different parameters on the PDIV can be studied. Additionally, partial

N. Driendl, F. Pauli and K. Hameyer are with the Institute of Electrical Machines, RWTH Aachen University, 52062 Aachen, Germany.

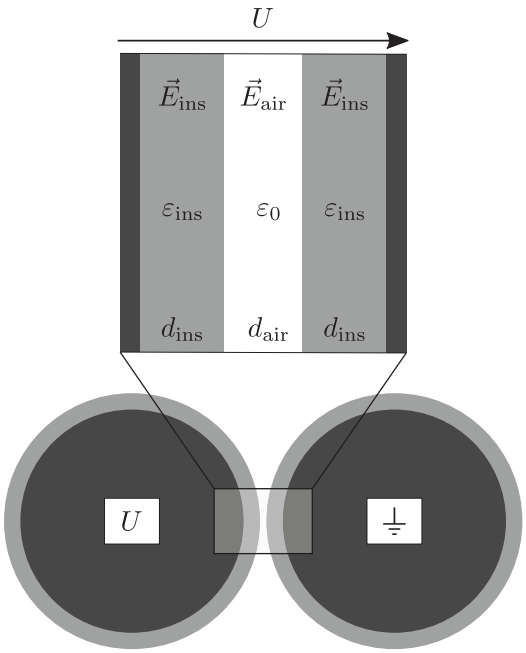

Fig. 1: Derivation of a simplified plane capacitor set up from the cross-section of a twisted pair.

discharge tests are conducted. By comparing both, the simulated and measured results, the secondary-electron-emission coefficient can be parameterized.

II. Technical Background

In this section, the influence of the insulation's material parameter on the electric field in air enclosures between adjacent wires is explained. Furthermore, the conditions for the inception of partial discharges is explained based on the *Townsend* criterion.

A. Permittivity and Insulation Thickness

For the insulation thickness and permittivity, the influence can be illustrated by the example of a plane capacitor as depicted in Fig. 1. In this example, the external voltage U is composed as follows:

$$U = E_{\mathrm{ins}} \cdot d_{\mathrm{ins}} + E_{\mathrm{air}} \cdot d_{\mathrm{air}} + E_{\mathrm{ins}} \cdot d_{\mathrm{ins}}. \tag{1}$$

With the boundary condition of the electric flux density D (2), the electric field E_{air} can be expressed depending on the insulation's material parameters (3):

$$D = \text{const.} \Rightarrow \varepsilon_{\mathrm{ins}} \cdot E_{\mathrm{ins}} = \varepsilon_0 \cdot E_{\mathrm{air}}, \tag{2}$$

$$E_{\mathrm{air}} = \frac{U}{2 \cdot d_{\mathrm{ins}} \cdot \frac{\varepsilon_{\mathrm{air}}}{\varepsilon_{\mathrm{ins}}} + d_{\mathrm{air}} \cdot \varepsilon_0}. \tag{3}$$

From this equation, it can be derived, that the electric field in air is increased by a higher permittivity $\varepsilon_{\mathrm{ins}}$ or a lower insulation thickness d_{ins}. The permittivity ε is specified as the product of the material-dependent relative permittivity ε_{r} and the vacuum permittivity ε_0:

$$\varepsilon = \varepsilon_{\mathrm{r}} \cdot \varepsilon_0. \tag{4}$$

B. Townsend Criterion

The *Townsend* criterion can be used to describe gas discharge processes. In general, during a gas discharge process, the conductivity of the gas increases due to collision processes and photo ionization where neutral gas atoms are split up into negative and positive charge carriers. These processes occur, if a starting electron has sufficient kinetic energy to ionize a gas molecule. Through this process, electrons are removed from the gas molecule moving in the direction of the anode. These electrons trigger further collision processes and cause an avalanche-like increasing amount of electrons on the way from cathode to anode. The residual positive ions left behind after the collision processes move in the opposite direction hitting the cathode material. Besides, photons are emitted by the ionization processes and also effect the cathode. Thereby, further starting electrons can be generated causing subsequent electron avalanches. According to *Townsend*, the ignition condition is fulfilled, if each avalanche triggers at least one avalanche. This condition is given by the following equation:

$$\gamma \cdot \left[\exp\left(\int_{x=0}^{d} \alpha_{\mathrm{eff}} \left(E(x) \right) \cdot \mathrm{d}x \right) - 1 \right] \geq 1. \tag{5}$$

In this equation, γ indicates the cathode reaction, i.e. released electrons by impacting positive ions and photons. This coefficient is also named secondary-electron-emission coefficient. Besides, other effects like ion emission and field emission are considered. α_{eff} is the effective ionization coefficient depending on the local electric field and d is the distance of the electrodes. The ionization coefficient indicates the number of new electrons generated by one electron per unit length and is dependent on the electric field strength. This formulation is valid for the inhomogeneous field [20].

C. Secondary-Electron-Emission Coefficient

The coefficient γ indicates several effects and depends on parameters like cathode material, gas, electric field and pressure. The specification of values for this coefficient varies greatly depending on the experimental conditions. Values for γ are specified for several metallic cathode materials and gases [20].

III. Determination of Relative Permittivity

In this paper, three different wires are examined. The first one is a commercially available wire with two insulation layers: PESI and PAI. The second one is insulated with a layer of of corona-resistant polyamide-imide (CR-PAI). The insulation layer of the third wire is composed of PEEK. In

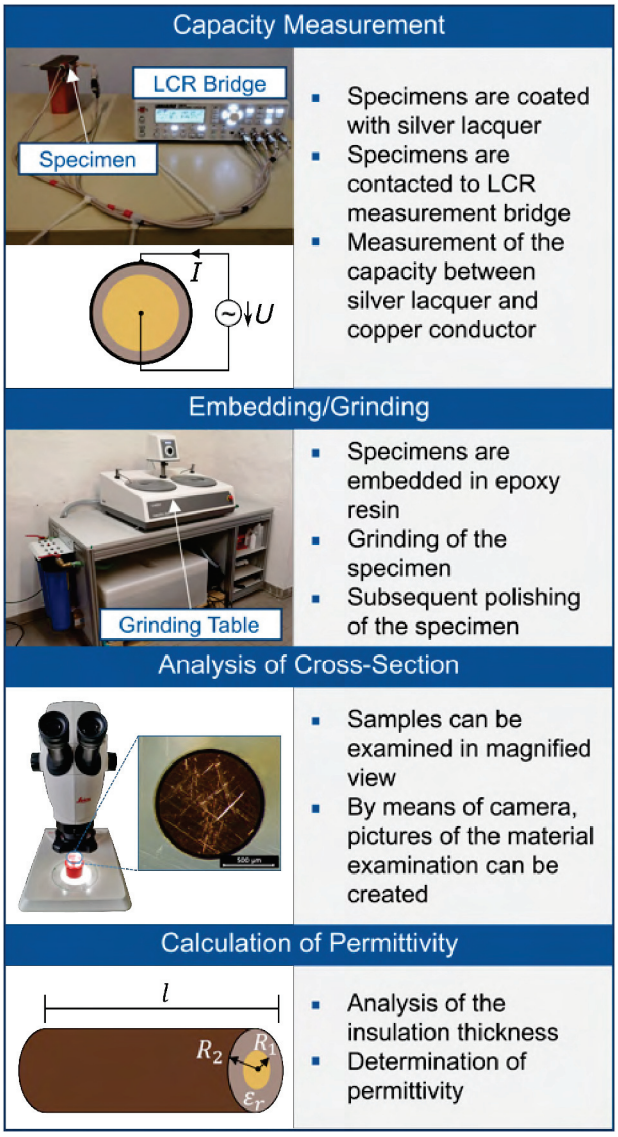

Fig. 2: Working steps to determine the permittivity.

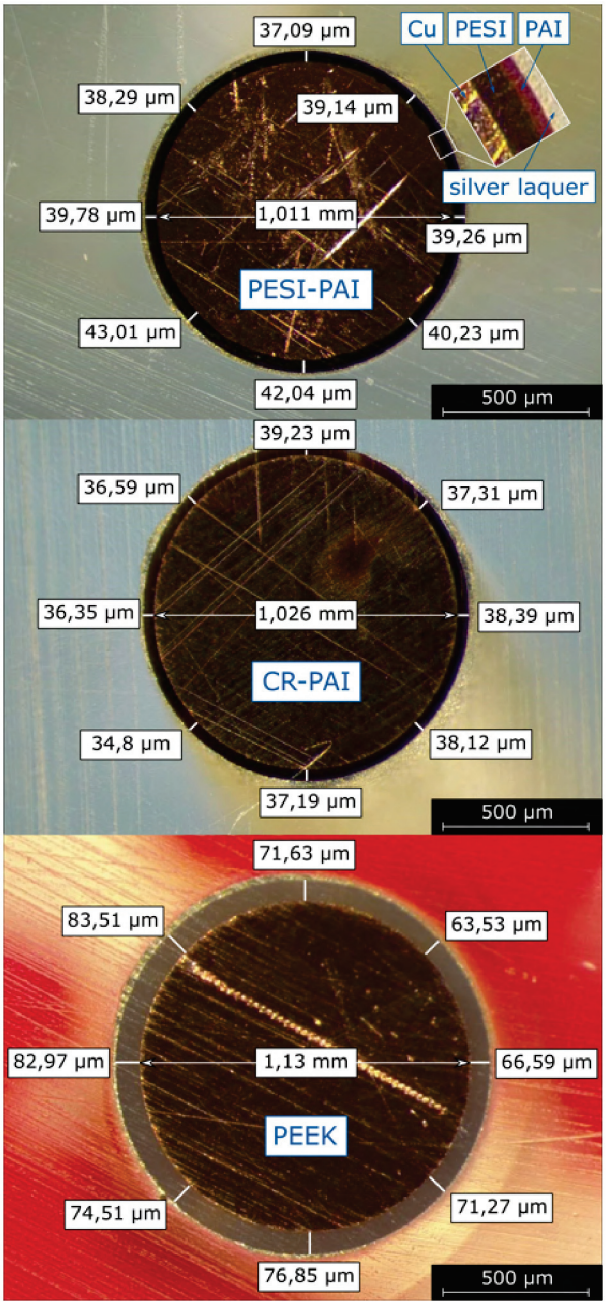

Fig. 3: Cross-section of wires.

TABLE I: Data of examined wires.

Insulation layer 1	Insulation layer 2	Insulation thickness
THEIC-modified polyester or polyesterimid	PAI	Grade 2
CR-PAI	-	Grade 2
PEEK	-	approx. 75 µm

the following, the wires are named according to the insulation layers. The first two wires are subject to the delivery conditions according to IEC 60317-0-1 [21]. This standard prescribes a minimum increase of the wire diameter due to the insulation layer as well as a maximum outer diameter. For a Grade 2 wire with a diameter of 1 mm, the insulation thickness is within the limits of 31.5 µm and 47 µm. The third wire is a custom-made wire with an expected insulation thickness of 75 µm according to the manufacturer. The known data before examination are summarized in Table I.

The determination of the relative permittivity of the insulation layer $\varepsilon_{\mathrm{r,ins}}$ is composed of several steps as visualized in Fig. 2. The measurement principle is based on

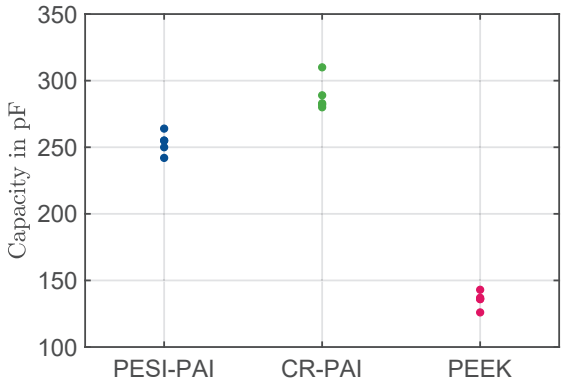

Fig. 4: Measurement of the capacity.

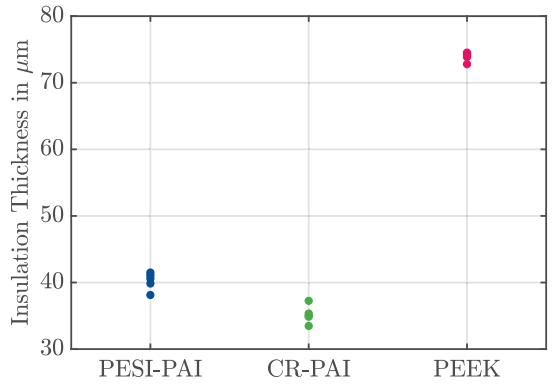

Fig. 5: Measurement of the insulation thickness.

a cylinder capacitor geometry. Firstly, the wires are coated with silver lacquer over a defined length of $10\,\mathrm{cm}$ forming an electrode at the surface of the insulation layer. This length corresponds to the prescribed value for the determination of the dissipation factor for enamelled copper wires according to IEC 60851-5 [22]. The second electrode is defined by the copper conductor itself. The capacity of the specimens is measured by means of an LCR-bridge (R&S®HM8118 Programmable LCR-Bridge) for a frequency of $50\,\mathrm{Hz}$. The results can be seen in Fig. 4. Subsequently, the wires are embedded in epoxy resin and processed by a grinding table. After that, the cross section of the different wires is examined with the aid of a microscope. An exemplary picture of each type of wire is shown in Fig. 3. To reduce deviations due to tilting of the specimens during the grinding process and deviations due to the manufacturing process, the thickness of the insulation layer is measured at eight different points. For further calculations, the mean value of the measurement points is considered. The results can be seen in Fig. 5. The mean values of the insulation layer thickness of the different wires are $40\,\mu\mathrm{m}$ (PESI-PAI), $35\,\mu\mathrm{m}$ (CR-PAI) and $74\,\mu\mathrm{m}$ (PEEK). It can be seen that the value of the PESI-PAI wire is in the middle of the expected value range, while the value of the CR-PAI wire is near the lower limit. This suggests the latter wire to have a lower PDIV. The PESI-PAI wire has two insulation layers, the inner layer being two and a half times the size of the outer layer. With the PEEK wire, it is noticeable that the insulation layer is not concentric to the conductor. The mean value of the insulation thickness is above the maximum value of a grade 3 wire.

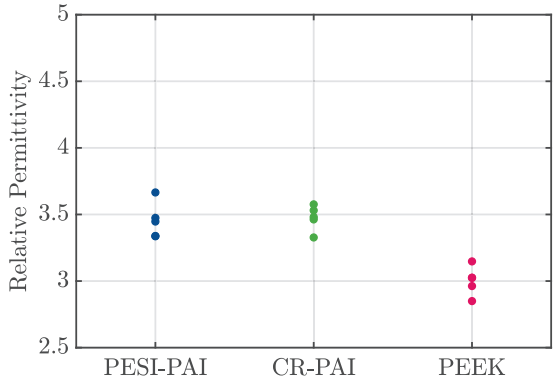

Fig. 6: Calculated relative permittivity.

With the help of the available measurement results, the permittivity can now be calculated:

$$\varepsilon_\mathrm{r} = \frac{C}{2\pi\varepsilon_0 l} \ln\left(\frac{R_2}{R_1}\right). \tag{6}$$

In eq. (6), C is the measured capacity, l the length of the electrode, R_1 the copper radius and R_2 the copper radius plus the insulation thickness. Fig. 6 shows the results of the calculated relative permittivity.

IV. Application of the Townsend Criterion

In this section, the *Townsend* criterion is used to characterize partial discharge processes in the twisted pair arrangement. These occur inside air between the insulation surfaces. In the first step, a model is set up to get the voltage distribution and the electric field by a simulation according to the finite element method. The input parameter of the simulation are voltage U, conductor radius r_cond, insulation thickness d_ins and permittivity of the insulation ε_ins. Additionally, a minimum distance of $2\,\mu\mathrm{m}$ is introduced between the wires for numerical reasons. The electric field distribution for the three wires can be seen in Fig. 7. For a qualitative comparison, a voltage of $1\,\mathrm{V}$ is applied. It is shown that the electric field inside the air gap is significantly higher in an arrangement with a thinner insulation wire (PESI-PAI and CR-PAI). This study is consistent with eq. (3). The PESI-PAI wire consists of two insulation layers with different values of permittivity. With this method, only an effective value for both layers can be considered. The application of the *Townsend* criterion on the simulation model is sketched in Fig. 8. In the upper part, the two-dimensional equivalent arrangement including exemplary field lines inside air is shown. It is worth mentioning that the actual field lines

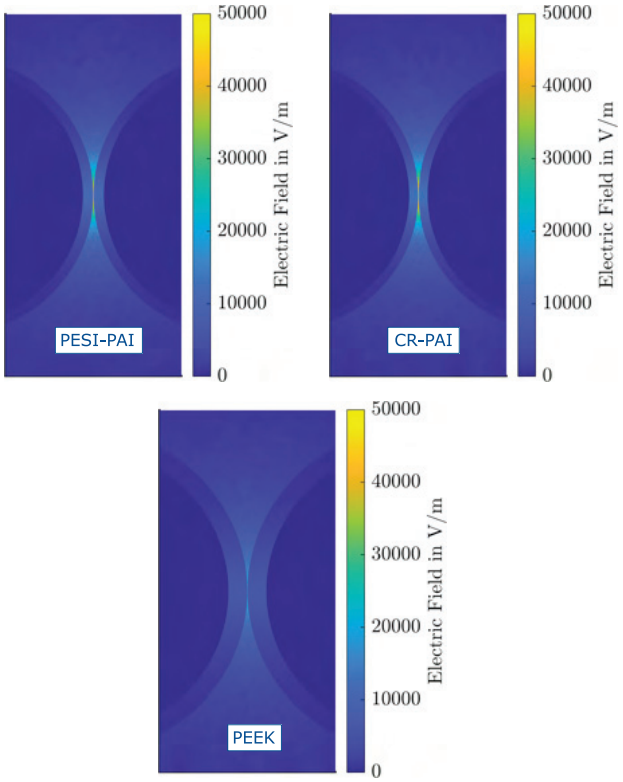

Fig. 7: Comparison of electric field distribution.

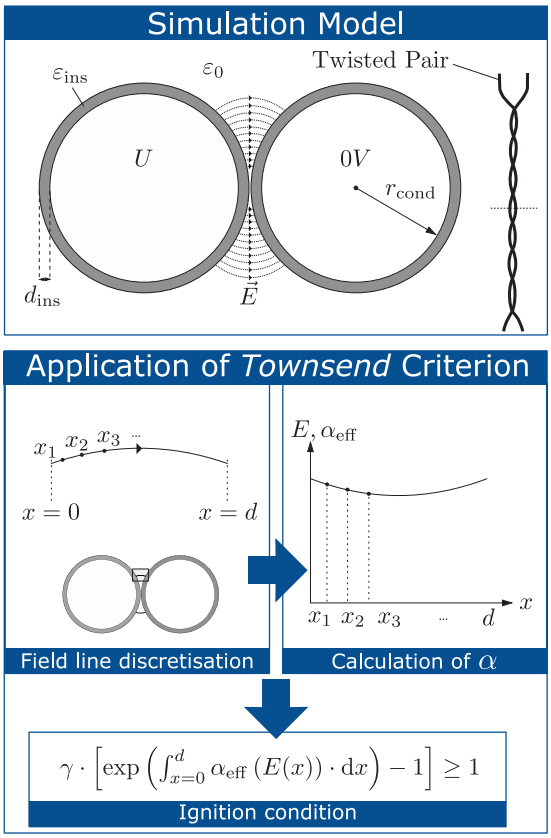

Fig. 8: Schematic representation of the simulation model.

end at the conductor surfaces. For modelling gas discharge processes, only the field inside the air is relevant. By knowing the electric field strength inside air, the *Townsend* criterion can be applied for field lines between the insulation surfaces. This procedure is shown in the lower part of Fig. 8. Each field line is sampled along its length in discrete steps. The ionization coefficient is calculated depending on the electric field. The secondary-electron-emission *Townsend* coefficient is initially set to 0.001. The final value is later determined for each wire based on partial discharge tests. The input voltage is varied until the ignition condition is fulfilled for one field line which is named critical field line.

At a low-frequency sinusoidal voltage, the corresponding peak value of the voltage is regarded to be the PDIV. For impulse voltage with steep voltage slopes and a strong overshoot behaviour, other effects have to be considered [23]. The application of the *Townsend* criterion is illustrated in Fig. 8. For each considered field line, yields the following results: 1051 V (PESI-PAI wire), 1012 V (CR-PAI wire) and 1402 V (PEEK wire). The simulated PDIV of the CR-PAI wire is slightly lower than the PDIV of the PESI-PAI wire which can be explained by the lower insulation thickness. The results of the PEEK wire correspond to the expectation that the PDIV is significantly higher for a thicker insulation layer and a lower permittivity.

V. Partial Discharge Measurement

To study the influence of the material parameters of the insulation on the PDIV, partial discharge measurements

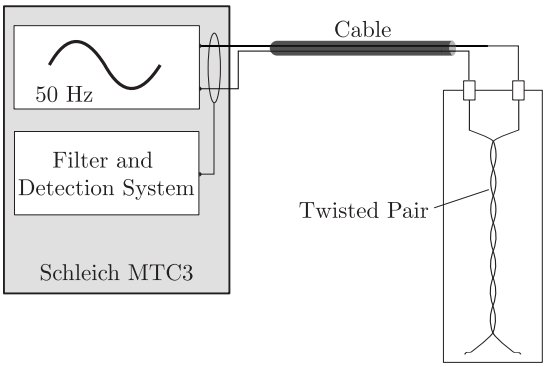

Fig. 9: Setup for partial discharge measurements.

are carried out. For each type of wire, twisted pairs are manufactured according to IEC 60172 [24]. Among other things, this standard prescribes the number of twists and the load weight during the twisting process. Subsequently, the specimens are subjected to heat storage at 100 °C for 24 h to remove impurities. For the measurement of the PDIV, a commercial stator tester (*Schleich MTC 3*) is used. This device allows standardized measurements according to IEC/TS 61934 [25]. The measurement setup is shown in Fig. 9.

In inverter-driven electrical machines, impulse voltages occur at the machine's terminals with a certain frequency. Besides the frequency of the pulse width modulation, other

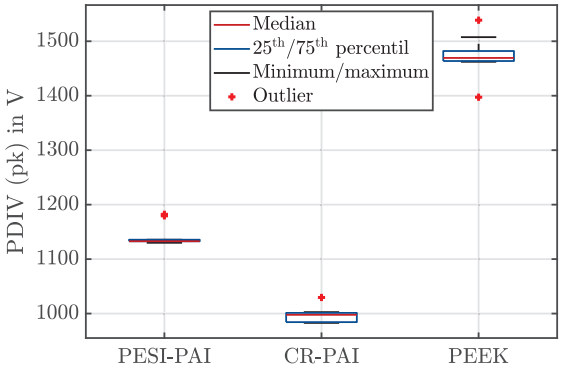

Fig. 10: Partial discharge measurement results for sinusoidal voltage (50 Hz).

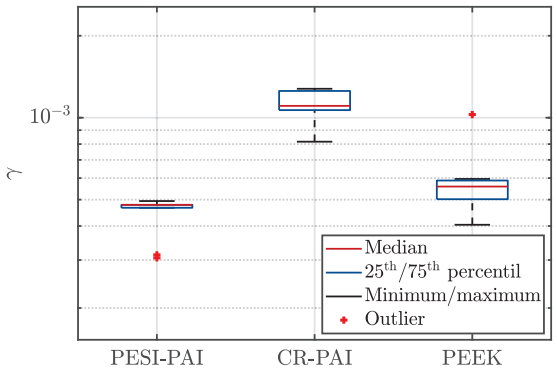

Fig. 11: Calculated secondary-electron-emission coefficient.

frequencies are emitted due to the steep voltage slopes. To study the material influence at a defined frequency, a sinusoidal test voltage is more suitable. Therefore, the PDIV is measured at a sinusoidal voltage of 50 Hz. The results can be seen in Fig. 10 and refer to the peak (pk) voltage of the test voltage. The results of the PESI-PAI wire are 1142 V for the mean value and 20 V for the standard deviation of the PDIV, respectively. The calculated value of 1051 V is 8 % below the measured mean value. For the CR-PAI wire, the mean value of the measured PDIV is 996 V which is very close to the simulated value of 1012 V. The standard deviation of the measured PDIV is 14 V. The results of the PEEK wire show the highest standard deviation of 35 V with a mean value of 1474 V. The comparatively high deviation of the measurement results can be attributed to the non-concentric position of the conductor inside the insulation layer. Regarding the cross section of two adjacent wires, different values for the insulation thickness can occur influencing the measured PDIV. The calculated value for the PDIV is 5 % below the measured one.

VI. Determination of the Secondary-Electron-Emission Coefficient

The comparison of the simulated and measured values of the PDIV shows some deviations. These can be attributed to differences of the coefficient γ for the insulation materials. As mentioned in Section IV, the initial value is set to 0.001. With the measurement results, γ can be calculated by applying the ignition condition eq. (5). Specifically, the parameter γ is varied, until a field line is found at which the ignition condition is fulfilled for the corresponding PDIV value.

The results are shown in Fig.11. Due to the exponential correlation of the measurement results and the secondary-electron-emission coefficient, small deviations in the PDIV result in large deviations of γ. It has to be noticed that this method should be seen as an estimation. In this two-dimensional arrangement, parameter like $d_{\min}$ also influence the results. Twisted pairs are used to best represent the turn-to-turn insulation by ensuring a contact of the insulation surfaces which is regarded to be the worst-case scenario. To improve the accuracy of the determination of γ, the distance of the insulation surfaces and the location of the discharge process should be known exactly.

By qualitatively comparing the results, the CR-PAI wire has significantly larger values for γ than the PESI-PAI wire where PAI is the outer insulation layer. This leads to the assumption that the corona-resistant nano-fillers lead to easier detrapping of electrons from the insulation surface.

VII. Conclusions

In this work, a method to study the influence of insulation material's parameters is presented. To determine the permittivity of the material, capacity measurements on different wires are carried out. To allow capacity measurements of the insulation layer, the surface is coated with silver lacquer. Subsequently, the cross-section of the wires is analysed to determine the thickness of the insulation layers. With these parameters, the permittivity can be calculated analogous to a cylindrical capacitor.

For the three different wires, a simulation model is set up to study the influence of different parameters and to calculate the expected PDIV. For both grade 2-wires (PESI-PAI and CR-PAI), the PDIV is expected to be in the same range. However, the simulated PDIV of the CR-PAI wire is slightly smaller because of the smaller insulation thickness. The permittivity is in the same range for both wires. The simulated PDIV of the PEEK wire is almost 50 % higher than the PDIV of the grade 2-wires. The main reason is the significantly greater insulation layer thickness. Another reason is the lower value of the permittivity.

The PDIV is measured for each type of wire by using twisted pairs with a sinusoidal test voltage. The expectations based on the measurement results are qualitatively confirmed. Quantitatively, the comparison of the simulated and measured results shows differences which can be attributed to the secondary-electron-emission coefficient. Therefore, the ignition condition for gas discharge processes is used to

determine this parameter depending on the measurement results.

REFERENCES

[1] M. Chapman, N. Frost, and R. Bruetsch, "Insulation systems for rotating low-voltage machines," in *Conference Record of the 2008 IEEE International Symposium on Electrical Insulation*, 2008, pp. 257–260.

[2] B. Florkowska, J. Roehrich, P. Zydron, and M. Florkowski, "Partial discharge characteristics of enameled wire of electric machine winding under exploitation stresses," in *2010 10th IEEE International Conference on Solid Dielectrics*, 2010, pp. 1–4.

[3] Q. Khan, S. S. Refaat, H. Abu-Rub, and H. A. Toliyat, "Partial discharge modeling of internal discharge in electrical machine stator winding," in *2020 IEEE Kansas Power and Energy Conference (KPEC)*, 2020, pp. 1–6.

[4] D. Fabiani, G. Montanari, A. Cavallini, and G. Mazzanti, "Relation between space charge accumulation and partial discharge activity in enameled wires under pwm-like voltage waveforms," *IEEE Transactions on Dielectrics and Electrical Insulation*, vol. 11, no. 3, pp. 393–405, 2004.

[5] *Rotating electrical machines - Part 18-41: Partial discharge free electrical insulation systems (Type I) used in rotating electrical machines fed from voltage converters – Qualification and quality control tests*, IEC Standard 60 034-18-41 ed. I, November 2014.

[6] M. Melfi, J. Sung, S. Bell, and G. Skibinski, "Effect of surge voltage risetime on the insulation of low voltage machines fed by pwm converters," in *IAS '97. Conference Record of the 1997 IEEE Industry Applications Conference Thirty-Second IAS Annual Meeting*, vol. 1, 1997, pp. 239–246 vol.1.

[7] S. Mahdavi and K. Hameyer, "High frequency equivalent circuit model of the stator winding in electrical machines," in *2012 XXth International Conference on Electrical Machines*, 2012, pp. 1706–1711.

[8] R. Maier and M.-M. Bakran, "SiC effect on surge voltage distribution in large electrical machines," in *PCIM Europe 2018; International Exhibition and Conference for Power Electronics, Intelligent Motion, Renewable Energy and Energy Management*, 2018, pp. 1–7.

[9] S. Grubic, J. M. Aller, B. Lu, and T. G. Habetler, "A survey on testing and monitoring methods for stator insulation systems of low-voltage induction machines focusing on turn insulation problems," *IEEE Transactions on Industrial Electronics*, vol. 55, no. 12, pp. 4127–4136, 2008.

[10] Y. Yagami, C. Araki, Y. Mizuno, and H. Nakamura, "Diagnosis of turn-to-turn insulation failure of induction motor winding with aid of support vector machine," in *2014 IEEE Conference on Electrical Insulation and Dielectric Phenomena (CEIDP)*, 2014, pp. 445–448.

[11] V. Madonna, P. Giangrande, W. Zhao, Y. Wang, H. Zhang, and M. Galea, "Insulation capacitance as diagnostic marker for thermally aged, low voltage electrical machines," in *2019 22nd International Conference on Electrical Machines and Systems (ICEMS)*, 2019, pp. 1–5.

[12] F. Aymonino, T. Lebey, D. Malec, C. Petit, J. S. Michel, and A. Anton, "Dielectrics measurements of rotating machines insulation at high temperature (200-400°c)," in *2006 IEEE Conference on Electrical Insulation and Dielectric Phenomena*, 2006, pp. 740–743.

[13] A. Rumi, J. G. Marinelli, P. Seri, M. Kohler, and A. Cavallini, "Performance of corona resistant insulation for aerospace," in *2021 IEEE Electrical Insulation Conference (EIC)*, 2021, pp. 22–25.

[14] M. Hikita, K. Yamaguchi, M. Fujimoto, M. Kozako, S. Ohtsuka, M. Ohya, K. Tomizawa, and N. Fushimi, "Partial discharge endurence test on several kinds of nano-filled enameled wires under high-frequency ac voltage simulating inverter surge voltage," in *2009 IEEE Conference on Electrical Insulation and Dielectric Phenomena*, 2009, pp. 719–722.

[15] X. Xia, J. Yin, G. Li, and C. Liu, "Study on the corona resistant property of polymide/TiO2@SiO2 films," in *Ifost*, vol. 1, 2013, pp. 101–104.

[16] N. Hayakawa and H. Okubo, "Partial discharge characteristics of inverter-fed motor coil samples under ac and surge voltage conditions," *IEEE Electrical Insulation Magazine*, vol. 21, no. 1, pp. 5–10, 2005.

[17] N. Yanaze, H. Nakaya, M. Kozako, M. Hikita, K. Tomizawa, and M. Ohya, "Partial discharge inception voltage measurement and location identification of enamel coating ribbon wire used for low-voltage motors," in *2014 IEEE Conference on Electrical Insulation and Dielectric Phenomena (CEIDP)*, 2014, pp. 192–195.

[18] K. Maeda, T. Kubo, T. Uchimura, H. Mizoguchi, M. Kozako, M. Hikita, H. Fukuda, D. Mutou, K. Tomizawa, and K. Ikeda, "Partial discharge inception voltage of enameled cellular wire under impulse voltage," in *2018 IEEE 2nd International Conference on Dielectrics (ICD)*, 2018, pp. 1–6.

[19] P. Collin, D. Malec, and Y. Lefevre, "About the relevance of using paschen's criterion for partial discharges inception voltage (pdiv) estimation when designing the electrical insulation system of inverter fed motors," in *2019 IEEE Electrical Insulation Conference (EIC)*, 2019, pp. 513–516.

[20] A. Küchler, *High Voltage Engineering: Fundamentals - Technology - Applications*, ser. VDI book. Springer Berlin Heidelberg, 2017.

[21] *Specifications for particular types of winding wires – Part 0-1: General requirements - Enameled round copper wire*, IEC Standard 60 317-0-1, 2013.

[22] *Winding wires – Test methods – Part 5: Electrical properties*, IEC Standard 60 851-5, 2008.

[23] N. Driendl, F. Pauli, and K. Hameyer, "Modeling of partial discharge processes in winding insulation of low-voltage electrical machines supplied by high du/dt inverters," in *IECON 2019 - 45th Annual Conference of the IEEE Industrial Electronics Society*, vol. 1, 2019, pp. 7102–7107.

[24] *Test procedure for the determination of the temperature index of enamelled and tape wrapped winding wires*, IEC Standard 60 172, 2015.

[25] *Electrical insulating materials and systems – Electrical measurement of partial discharges (PD) under short rise time and repetitive voltage impulses*, IEC/TS Standard 61 934, 2011.

VIII. BIOGRAPHIES

Niklas Driendl received the M.Sc. degree in electrical engineering from RWTH Aachen University, Germany, in October 2018. He started working as a research associate at Institute of Electrical Machines in January 2019. His research interests are the characterization of insulation systems of electrical machines and modeling of partial discharge processes.

Florian Pauli received the M.Sc. degree in electrical engineering from RWTH Aachen University, Germany, in April 2017. He has been working as a research associate at the Institute of Electrical Machines since May 2017. His research interests include iron loss computations, thermal behavior, overload capability, lifetime models and the characterization of insulation systems of electrical machines.

Kay Hameyer (IEEE M96 - SM99) received the M.Sc. degree in electrical engineering in 1986 from the University of Hannover, Germany, 1992 his Ph.D. degree from University of Technology Berlin, Germany for working on permanent magnet excited machines. After his university studies he worked with the Robert Bosch GmbH in Stuttgart, Germany, as a design engineer for permanent magnet servo motors. From 1988 to 1993 he was a member of staff at the University of Technology Berlin, Germany. From 1996 to 2004, he was then a Full Professor of Numerical Field Computations and Electrical Machines, Katholieke Universiteit Leuven (KU Leuven), Leuven, Belgium. Since 2004, he has been a Full Professor and the Director of the Institute of Electrical Machines (IEM), RWTH Aachen University, Aachen, Germany. His research interest focuses on all aspects of the design, control and manufacturing of electrical machines and the associated numerical simulation. The characterization and modeling of hard- and soft-magnetic materials is another focus of his work. He has authored/coauthored more than 350 journal publications, more than 700 international conference publications and four books. His research interests include numerical field computation and optimization, the design and control of electrical machines, in particular, permanent-magnet excited machines, induction machines. Dr. Hameyer is a member of the German VDE, a senior member of IEEE and a Fellow of the Institution of Engineering and Technology, U.K.